

RESEARCH ARTICLE

Optimization of Electroencephalogram Feature Based on Multi-Band Feature Matrix and Relative Difference for Imagined Motor Movement Pattern Classification

I Made Agus Wirawan^{1,*} , I Nyoman Sukajaya²  and Ni Nyoman Mestri Agustini³ ¹*Department of Informatics Engineering, Universitas Pendidikan Ganesha, Indonesia*²*Department of Mathematics, Universitas Pendidikan Ganesha, Indonesia*³*Department of Neurology and Medical Rehabilitation, Universitas Pendidikan Ganesha, Indonesia*

Abstract: Electroencephalogram (EEG)-based imagined motor movement recognition plays a crucial role in brain–computer interface applications and medical rehabilitation systems. However, EEG signals inherently exhibit high levels of noise, are nonlinear and nonstationary, contain spatial information, and show significant signal pattern variance across individuals, complicating feature extraction and classification. This study proposes a novel framework that integrates the relative difference method with a multi-band feature matrix, explicitly incorporating four EEG frequency bands (theta, alpha, beta, and gamma) mapped according to the international system 10–20. The extracted features are processed by a three-layer convolutional neural network (CNN) for classification. The proposed method is evaluated on the MIMED dataset for six-class imagined motor movement recognition and validated on the AMIGOS dataset for four-class emotion recognition. The experimental evaluation on the MIMED dataset demonstrates consistently strong classification performance, achieving 99.36% accuracy, 99.37% precision, 99.37% recall, and an F1-score of 99.36%. These results significantly outperform those without baseline reduction, the difference, and the fractional methods. Further validation on AMIGOS shows that the proposed model achieves an accuracy of 99.64%. This result surpasses the previously reported state of the art. These findings confirm that combining relative difference and multi-band feature matrices produces more stable, representative, and discriminative EEG features, making them readily recognizable by CNN methods. The proposed approach has strong potential for real-time brain–computer interfaces, clinical neurorehabilitation, and emotion-sensitive human–computer interaction systems.

Keywords: electroencephalogram, relative difference, multi-band feature matrix, brain-computer interface, imagined motor movement

1. Introduction

Recognizing imagined motor movement from electroencephalogram (EEG) signals has high potential for application across various fields, including brain–computer interfaces, medical rehabilitation, and the mechanisms of motor control [1]. This technology allows individuals with motor impairments, such as stroke or amyotrophic lateral sclerosis, to interact with external devices through imagined motor movement, without direct physical activity [2, 3]. Furthermore, using EEG signals to detect imagined motor movement can support neuroplasticity-based therapy in restoring patients' motor function [4, 5].

To improve the recognition performance of imagined motor movement patterns, several characteristics of the EEG signals are

essential to consider in generating optimal features and pattern recognition, such as containing high noise/artifacts, having spatial information between channels and frequency bands, being nonlinear, nonstationary, and having different signal pattern variations in everyone [6, 7]. To consider these characteristics, previous studies have reviewed various proposed methods for generating optimal features from EEG signals, using techniques based on the time, frequency, and time-frequency domains [7, 8]. Among these techniques, the differential entropy (DE) method is more accurate and stable at generating EEG signals features than others. In addition, DE-based feature extraction can be implemented on EEG signals represented in the time-frequency domain. In this approach, the signals are decomposed into four frequency bands associated with conscious brain activity, namely, theta, alpha, beta, and gamma [9, 10].

However, the DE method is unable to characterize differences in EEG signals patterns between individuals and reduce artifacts in EEG signals. Optimization studies of the DE method

*Corresponding author: I Made Agus Wirawan, Department of Informatics Engineering, Universitas Pendidikan Ganesha, Indonesia. Email: imade.aguswirawan@undiksha.ac.id

were conducted by combining it with the difference method to characterize differences in EEG signals patterns between individuals. The difference method is a baseline reduction approach that uses baseline signal features to reduce variance in trial signal patterns [11, 12]. Overall, there are three baseline reduction methods: difference, relative difference, and fractional difference. Of these three methods, the relative difference method is superior to the other two [13]. Furthermore, to reduce artifacts in EEG signals, the DE method is combined with the modified weighted mean filter (MWMF). The combination of DE, relative difference, and MWMF methods can produce optimal EEG signals features [13].

Although various optimizations have been applied to the DE method for feature extraction, it still cannot capture the nonlinear, nonstationary, and artifact-sensitive characteristics of EEG signals. To address these issues, several researchers have proposed a convolution-based feature extraction process that employs a three-dimensional (3D) convolutional neural network (CNN) [14, 15]. This approach has several advantages, including automatic feature extraction without manual feature engineering, the ability to extract spatially dimensional features, the ability of CNNs to capture nonlinear relationships unattainable by traditional methods, and the ability to reduce artifacts in EEG signals by learning directly from varied data.

However, the 3D convolution method proposed by several previous researchers has not accounted for spatial information across the four frequency bands [16]. Therefore, this study proposes a multi-band feature matrix method combined with the relative difference method for extracting EEG signals features. The multi-band feature matrix represents 3D convolution by combining four frequency bands: theta, alpha, beta, and gamma. Furthermore, the relative difference method is a baseline reduction method used to characterize the variance in EEG signals patterns between individuals. For classification, this study uses a CNN to classify six motor movements: standing, sitting, raising the right hand, lowering the right hand, raising the left hand, and lowering the left hand. To test this proposed model, this study uses the MIMED dataset. This dataset has several advantages, including that it consists of six everyday human movement activities [17]. Using the proposed multi-band feature matrix method combined with relative difference, optimal features can be

produced, thereby improving the accuracy of the CNN method in recognizing six motor movement activities.

2. Research Methodology

Based on the conducted investigation, this work introduces a relative difference approach to mitigate variability in EEG signals patterns, employs a multi-band feature matrix strategy for structured feature representation, and utilizes a CNN for feature learning and classification. The training and evaluation processes are performed using motor execution (ME) data from the MIMED dataset. Overall, the proposed framework is organized into seven sequential research phases, as illustrated in Figure 1.

Based on Figure 1, each stage of the research procedure is explained as follows.

2.1. MIMED dataset collection stage

The motor imagination and motor execution dataset (MIMED) is a collection of EEG data for six motor movements and motor imagination. However, for the model development and testing, this study used only ME data to recognize the imagined motor movement. The ME dataset contains labels for the six movement activities [17]. Table 1 presents a description of the ME dataset.

2.2. EEG signals separation

This stage divides the EEG recordings into two components: baseline and trial segments. The baseline segment corresponds to the participant's resting or neutral condition and is captured while the participant remains relaxed. In contrast, the trial segment reflects brain activity associated with the participant's six ME tasks. An example of this segmentation for channel AF3 in the first participant's first scenario is shown in Figure 2.

Overall, the segmentation process was applied to 14 EEG channels and 24 experimental scenarios. For illustration, in the AF3 channel for the first scenario, the signal data had a total duration of 11,904 samples (equivalent to 93 s). The data range from 1 to 384 Hz (green line) is the baseline EEG signals, representing the participant's neutral state, while the data range from

Figure 1
Research procedures

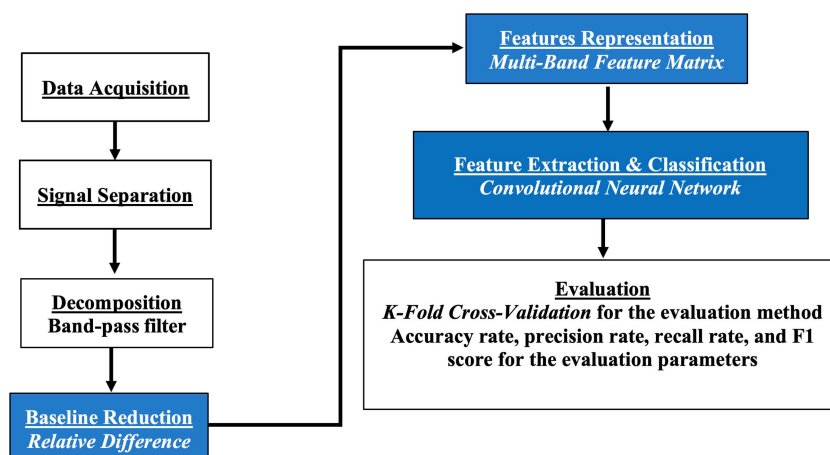


Table 1
Description of the motor execution dataset

No	Description	Remarks
1	Participants	30 people (16 men and 14 women)
2	Device	Emotiv EPOC X
3	Channel	14 channels
4	Sampling rate	128 Hz
5	Total data per participant	316,416
6	Number of scenarios	24 scenarios, consisting of raising the right hand, lowering the right hand, raising the left hand, lowering the left hand, standing, and sitting, each for two scenarios on the first day and two scenarios on the second day

Figure 2
Illustration of the EEG signals segmentation process for the AF3 channel in the first scenario from the first participant

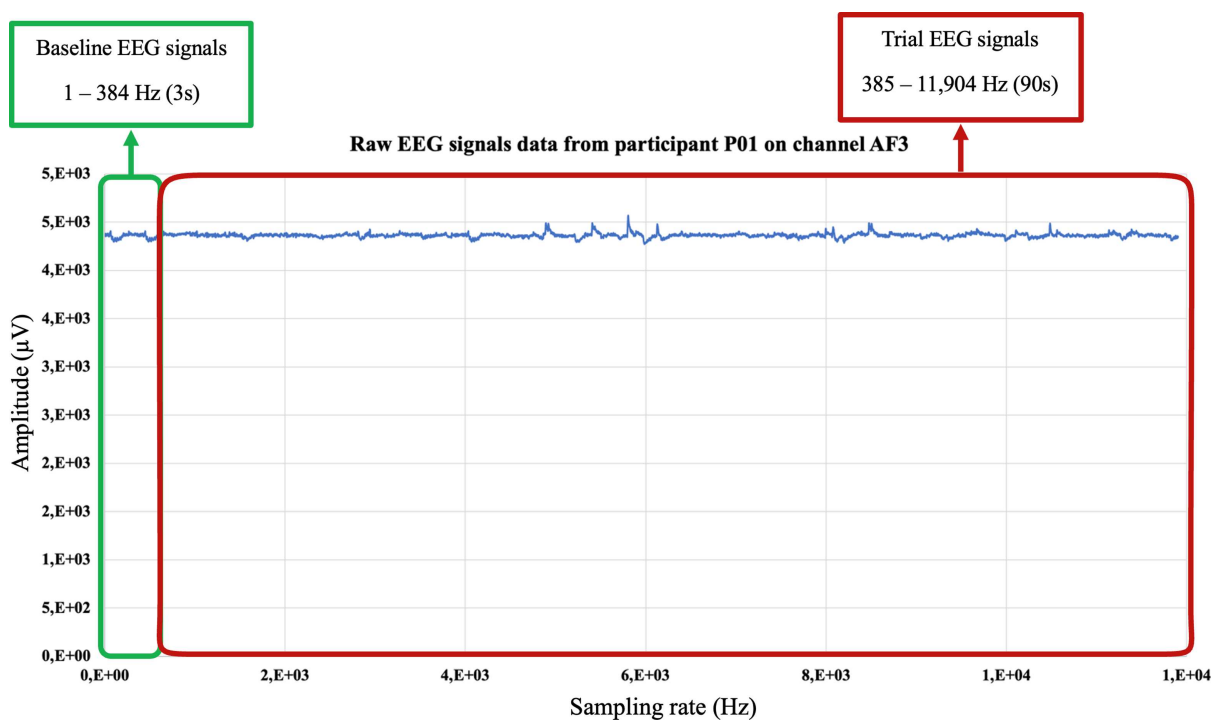


Table 2
The first three seconds of baseline EEG signals data for the AF3 channel in the first scenario

i^{th} Data	Baseline EEG signals (x_i)
1 Hz	x_1
2 Hz	x_2
.....
384 Hz	x_{384}

Table 3
Ninety seconds of trial EEG signals data for channel AF3 in the first scenario

i^{th} Data	Trial signal (x_k)
385 Hz	x_{385}
386 Hz	x_{386}
.....
11,904 Hz	$x_{11,904}$

385 to 11,904 Hz is the trial EEG signals, representing the participant's ME (red line). Table 2 presents an example of the baseline signal data for the first three seconds on the AF3 channel for the first scenario [17].

Furthermore, the trial EEG signals ranges from 385 Hz to 11,904 Hz (seconds 4–93). Table 3 presents the trial EEG signals data for channel AF3 in the first scenario.

2.3. Decomposition stage

In this stage, the EEG signals components are separated, both in baseline and trial conditions, into four leading frequency bands: theta (θ), alpha (α), beta (β), and gamma (γ).

This decomposition process aims to obtain a representation of the signal in each frequency band, as illustrated in Figure 3.

Figure 3
Four-frequency-band decomposition process

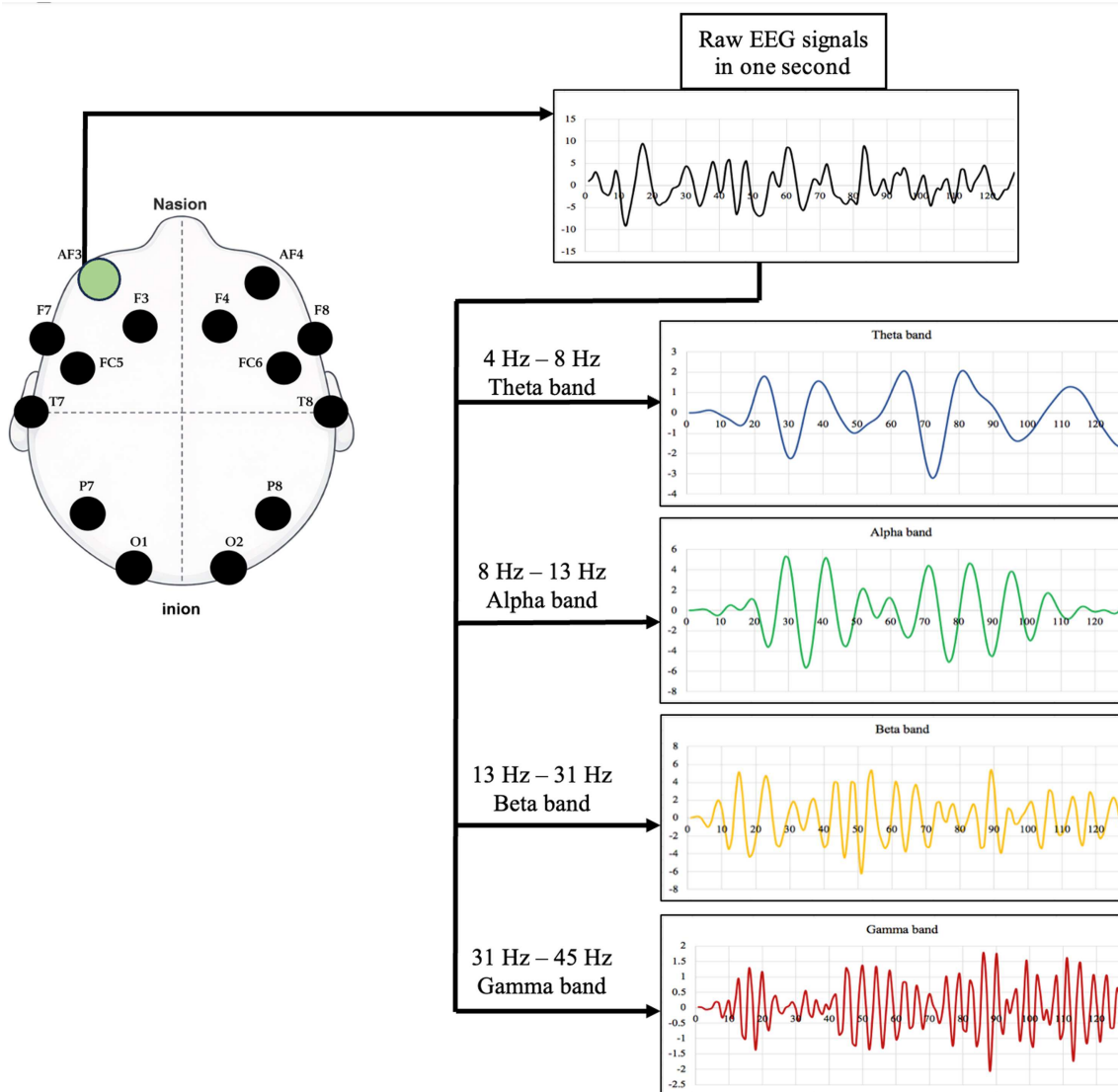


Table 4
Frequency-band decomposition process for a 3-second baseline EEG signals for channel AF3 in the first scenario

Frequency	Baseline EEG Signals			
	x_1	x_2	x_{384}
Theta band	$x(\theta)_1$	$x(\theta)_2$	$x(\theta)_{384}$
Alpha band	$x(\alpha)_1$	$x(\alpha)_2$	$x(\alpha)_{384}$
Beta band	$x(\beta)_1$	$x(\beta)_2$	$x(\beta)_{384}$
Gamma band	$x(\gamma)_1$	$x(\gamma)_2$	$x(\gamma)_{384}$

The EEG signals decomposition process was performed using a third-order Butterworth filter, with frequency filtering based on low-pass and high-pass bands that form a bandpass filter [12]. This filtering was applied to all scenarios, all channels, both baseline and trial signals.

Table 4 presents the results of the four-frequency-band decomposition for a 3-s baseline EEG signals (128 Hz) recorded from channel AF3 in the first scenario.

Table 5 presents 11,904 samples at a 90-s trial EEG signals (a sampling rate of 128 Hz) that has been decomposed into four frequency bands.

2.4. Baseline reduction stage

After the four frequency bands are obtained from the baseline and trial EEG signals, the next step is the baseline reduction

Table 5
Four-frequency-band decomposition process for a 90-s trial EEG signals for channel AF3 in the first scenario

Frequency	Trial EEG signals			
	x_{385}	x_{386}	$x_{11,904}$
Theta band	$x(\theta)_{385}$	$x(\theta)_{386}$	$x(\theta)_{11,904}$
Alpha band	$x(\alpha)_{385}$	$x(\alpha)_{386}$	$x(\alpha)_{11,904}$
Beta band	$x(\beta)_{385}$	$x(\beta)_{386}$	$x(\beta)_{11,904}$
Gamma band	$x(\gamma)_{385}$	$x(\gamma)_{386}$	$x(\gamma)_{11,904}$

process. This stage aims to generate feature values from the trial EEG signals that are more robust to signal pattern variability, potentially improving classification accuracy [13]. In this study, the relative difference method was used as the baseline reduction approach. Tables 6, 7, 8, and 9 present the results of the baseline reduction process using this method for the AF3 channel in the first scenario and the first participant.

Table 6
Illustration of baseline reduction calculations at theta frequencies using the relative difference method on the AF3 channel

Theta band	Baseline reduction
$f(\theta)_1$	$\frac{x(\theta)_{385}}{\text{mean}(x(\theta)_1, x(\theta)_{129}, x(\theta)_{257})}$
$f(\theta)_2$	$\frac{x(\theta)_{386}}{\text{mean}(x(\theta)_2, x(\theta)_{130}, x(\theta)_{258})}$
.....
$f(\theta)_{128}$	$\frac{x(\theta)_{512}}{\text{mean}(x(\theta)_{128}, x(\theta)_{256}, x(\theta)_{384})}$
.....
$f(\theta)_{11.520}$	$\frac{x(\theta)_{11,904}}{\text{mean}(x(\theta)_{128}, x(\theta)_{256}, x(\theta)_{384})}$

Table 7
Illustration of baseline reduction calculations at alpha frequencies using the relative difference method on the AF3 channel

Alpha band	Baseline reduction
$f(\alpha)_1$	$\frac{x(\alpha)_{385}}{\text{mean}(x(\alpha)_1, x(\alpha)_{129}, x(\alpha)_{257})}$
$f(\alpha)_2$	$\frac{x(\alpha)_{386}}{\text{mean}(x(\alpha)_2, x(\alpha)_{130}, x(\alpha)_{258})}$
.....
$f(\alpha)_{128}$	$\frac{x(\alpha)_{512}}{\text{mean}(x(\alpha)_{128}, x(\alpha)_{256}, x(\alpha)_{384})}$
.....
$f(\alpha)_{11.520}$	$\frac{x(\alpha)_{11,904}}{\text{mean}(x(\alpha)_{128}, x(\alpha)_{256}, x(\alpha)_{384})}$

Table 8
Illustration of baseline reduction calculations at beta frequencies using the relative difference method on the AF3 channel

Beta band	Baseline reduction
$f(\beta)_1$	$\frac{x(\beta)_{385}}{\text{mean}(x(\beta)_1, x(\beta)_{129}, x(\beta)_{257})}$
$f(\beta)_2$	$\frac{x(\beta)_{386}}{\text{mean}(x(\beta)_2, x(\beta)_{130}, x(\beta)_{258})}$
.....
$f(\beta)_{128}$	$\frac{x(\beta)_{386}}{\text{mean}(x(\beta)_{128}, x(\beta)_{256}, x(\beta)_{384})}$
.....
$f(\beta)_{11.520}$	$\frac{x(\beta)_{11,904}}{\text{mean}(x(\beta)_{128}, x(\beta)_{256}, x(\beta)_{384})}$

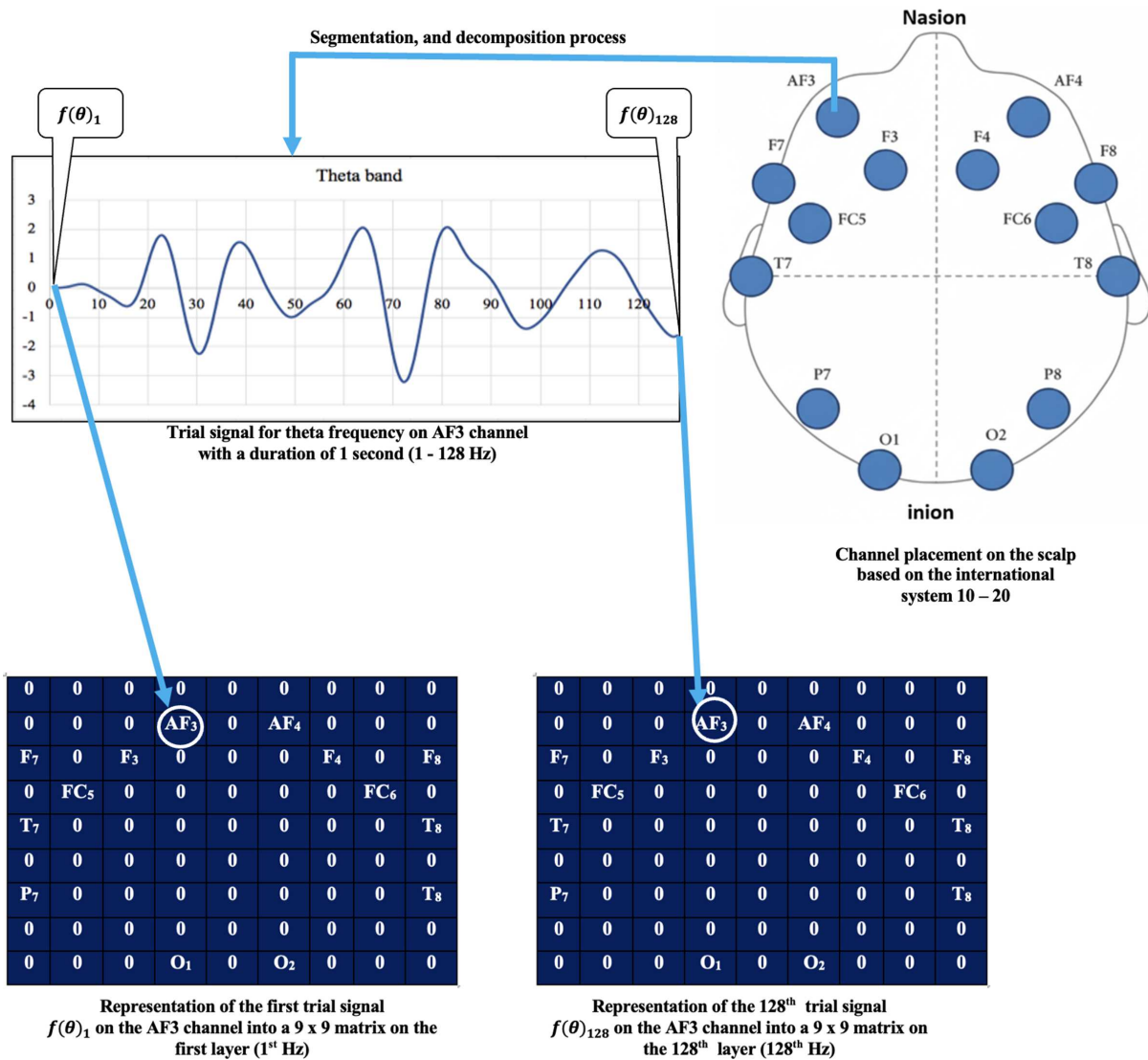
Table 9
Illustration of baseline reduction calculations at gamma frequencies using the relative difference method on the AF3 channel

Gamma band	Baseline reduction
$f(\gamma)_1$	$\frac{x(\gamma)_{385}}{\text{mean}(x(\gamma)_1, x(\gamma)_{129}, x(\gamma)_{257})}$
$f(\gamma)_2$	$\frac{x(\gamma)_{386}}{\text{mean}(x(\gamma)_2, x(\gamma)_{130}, x(\gamma)_{258})}$
.....
$f(\gamma)_{128}$	$\frac{x(\gamma)_{386}}{\text{mean}(x(\gamma)_{128}, x(\gamma)_{256}, x(\gamma)_{384})}$
.....
$f(\gamma)_{11.520}$	$\frac{x(\gamma)_{11,904}}{\text{mean}(x(\gamma)_{128}, x(\gamma)_{256}, x(\gamma)_{384})}$

2.5. Representation feature stage

The baseline-reduced EEG trial signal features are projected into a $9 \times 9 \times 512$ multi-band feature matrix structure according to the international system 10–20 [13]. The 9×9 matrix encodes the spatial distribution of scalp channels. At the same time, the 512 temporal-spectral dimension is obtained by concatenation of four frequency bands, each with 128 coefficients, as shown in Figure 4.

Figure 4
The process of representing 1st-second theta-frequency features on the AF3 channel in the $9 \times 9 \times 128$ feature matrix



Once all channels and frequency bands are represented, a multi-band feature matrix will be formed, as in Figure 5.

This representation is computed at 1-s intervals, yielding 128 features per frequency band across the four bands used. Each interval forms a multi-band feature matrix. In the first scenario, the EEG trial signals yielded 90 multi-band feature matrices, which were then used as input to the CNN architecture.

2.6. Feature extraction and classification stage

The CNN architecture used in this stage consists of four main components: convolution, flattening, feed-forward propagation, and backpropagation [12, 13].

The CNN architecture (Figure 6) consists of seven processes: the first convolution, the second convolution, the third convolution, flattening, the dense layer from the input node to the hidden node, the dense layer from the hidden node to the output node, and the backward process. The first and third convolutions use a 2×2 kernel, stride = 1, padding = same, and a Rectified Linear Unit (ReLU) activation function. Meanwhile, the softmax

activation function is applied from the hidden layer to the output layer [12, 13]. Details of the CNN architecture are shown in Table 10.

In the proposed CNN architecture, backpropagation is used to minimize a loss function formulated using categorical cross-entropy. Parameter updates are performed using the Adam optimization algorithm, which estimates first- and second-moment gradients to accelerate convergence and improve training stability.

2.7. Evaluation stage

To evaluate the contribution of the relative difference method combined with the multi-band feature matrix approach, this study designed four test scenarios. The first scenario applied the multi-band feature matrix without integrating the baseline reduction technique. The second scenario combined the multi-band feature matrix with the difference method; the third, with the relative difference method; and the fourth, with the fractional difference method. The implementation of these four scenarios aimed to

Figure 5
Feature representation process in a multi-band feature matrix

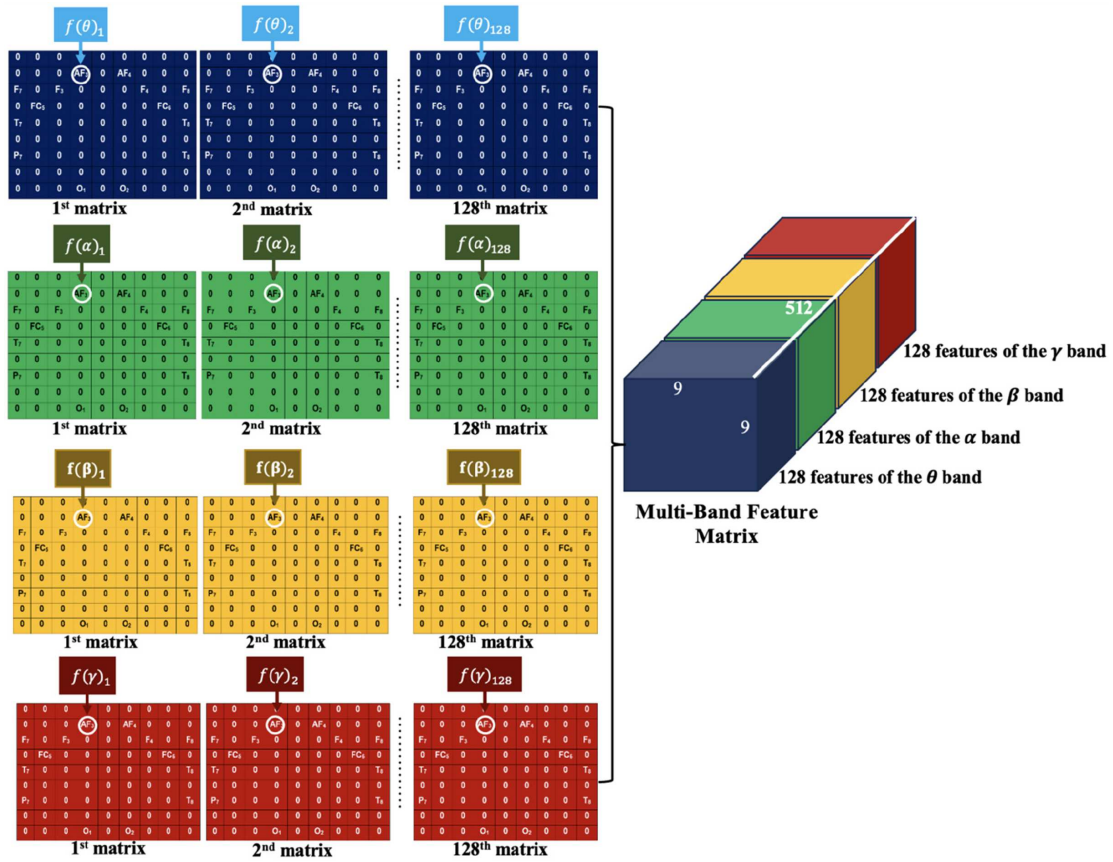


Figure 6
Illustration of the CNN architecture

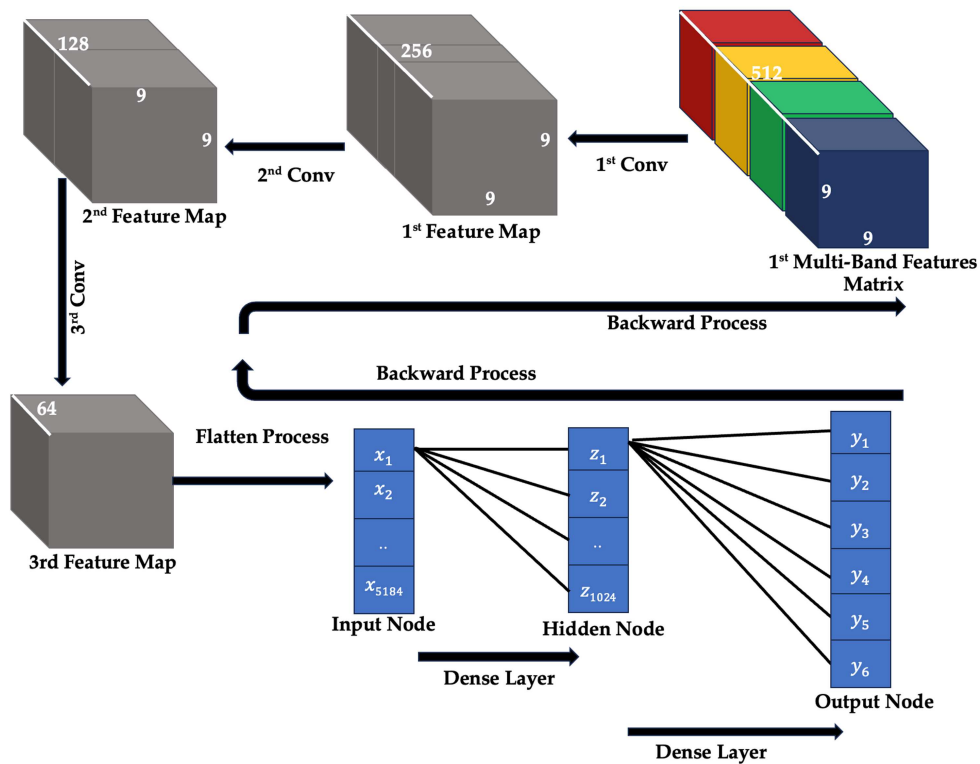


Table 10
Detailed CNN architecture and parameter count

No	Layer	Input shape	Output shape	Parameter count
1	Conv-1	$9 \times 9 \times 512$	$9 \times 9 \times 256$	524,544
2	Conv-2	$9 \times 9 \times 256$	$9 \times 9 \times 128$	131,200
3	Conv-3	$9 \times 9 \times 128$	$9 \times 9 \times 64$	32,832
4	Flatten	$9 \times 9 \times 64$	5184	–
5	Dense (hidden)	5184	1024	5,309,440
6	Dense (output)	1024	6	6,150
Total				6,004,166

validate the effectiveness of the relative difference in reducing artifacts in experimental EEG signals. Model performance was evaluated using a k-fold cross-validation scheme, with metrics including accuracy, precision, recall, and F1-score.

3. Results and Discussion

Based on four test scenarios conducted by independent subjects, the results for accuracy, precision, recall, and F1-score are as shown in Figures 7, 8, 9, and 10.

Figure 7 shows the classification model’s performance on six movement classes, optimized using the multi-band feature matrix method without baseline reduction. Overall, all evaluation metrics—accuracy, precision, recall, and F1-score—showed values below 20% for each participant. These results indicate that the model cannot effectively identify the six movement patterns without baseline reduction during feature extraction. Some participants, such as P10, P11, P22, and P25, performed slightly better than the others, but these values were still far below the expected level. This finding confirms that without baseline reduction, the features generated by the multi-band method lack sufficient representation power to classify the six movement classes accurately. Therefore, implementing baseline reduction is crucial for improving feature quality and classification performance.

The multi-band feature matrix approach combined with the difference method has been shown to yield a more optimal representation of EEG signals features, thereby improving classification accuracy. Performance evaluation based on four key

metrics—accuracy, precision, recall, and F1 score—showed very high and consistent performance, with average values exceeding 90% across all participants. The variance between parameters is relatively small, and although there is some variation in values, the overall performance remains in the outstanding category. These results indicate that applying the difference method to the EEG trial signal reduction stage significantly improved the quality of the EEG feature, which in turn led to a substantial increase in classification accuracy for the six movement classes compared to the first scenario (Figure 8). These findings underscore the crucial role of baseline reduction in EEG data preprocessing for optimizing classification performance.

In addition to the difference method, the multi-band feature matrix is also combined with the relative difference method. Based on the results shown in Figure 9, all evaluation parameters—accuracy, precision, recall, and F1 score—demonstrated very high performance, approaching the maximum value ($\pm 100\%$) in almost all participants. Only one participant (P11) had lower accuracy, precision, recall, and F1 score than the other participants (94.79% for accuracy, 95.09% for precision, 95.02% for recall, and 94.89% for F1 score). The findings suggest that participant P11 exhibits a comparatively higher level of artifacts than the other subjects. Nevertheless, despite being the lowest among all participants, P11’s accuracy, precision, recall, and F1-score each remain above 90%.

Overall, the consistently high scores across all metrics indicate that the relative difference method effectively improves the quality of the EEG feature, thereby significantly improving

Figure 7
Representation of accuracy, precision, recall, and F1-score values in the 1st scenario

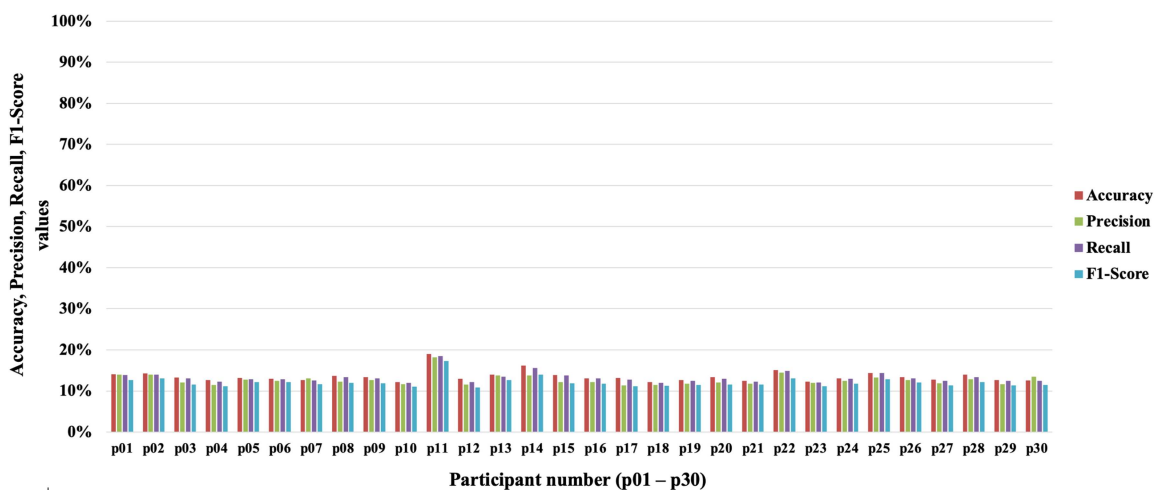


Figure 8
Representation of accuracy, precision, recall, and F1 score values in the 2nd scenario

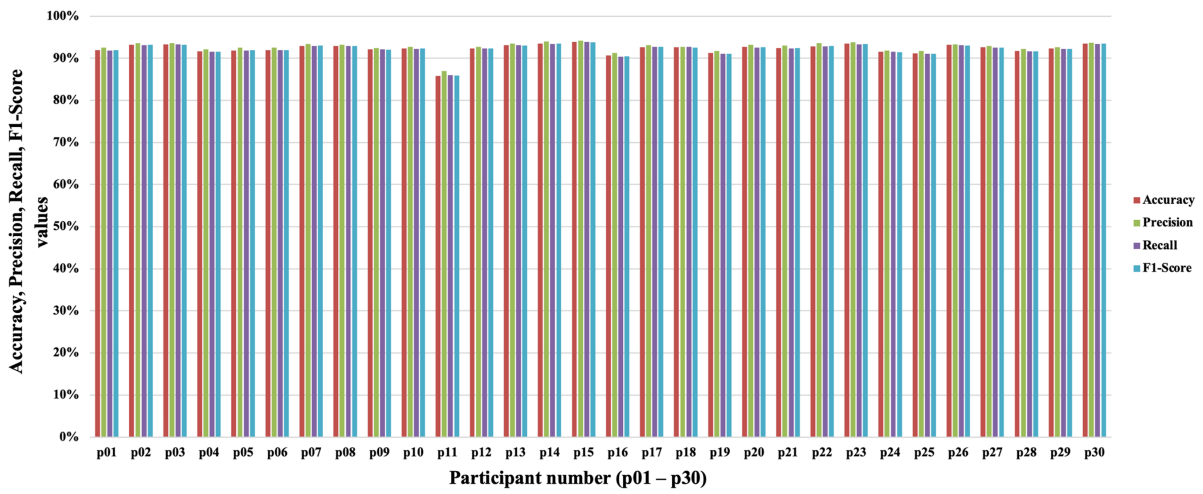


Figure 9
Representation of accuracy, precision, recall, and F1 score values in the 3rd scenario

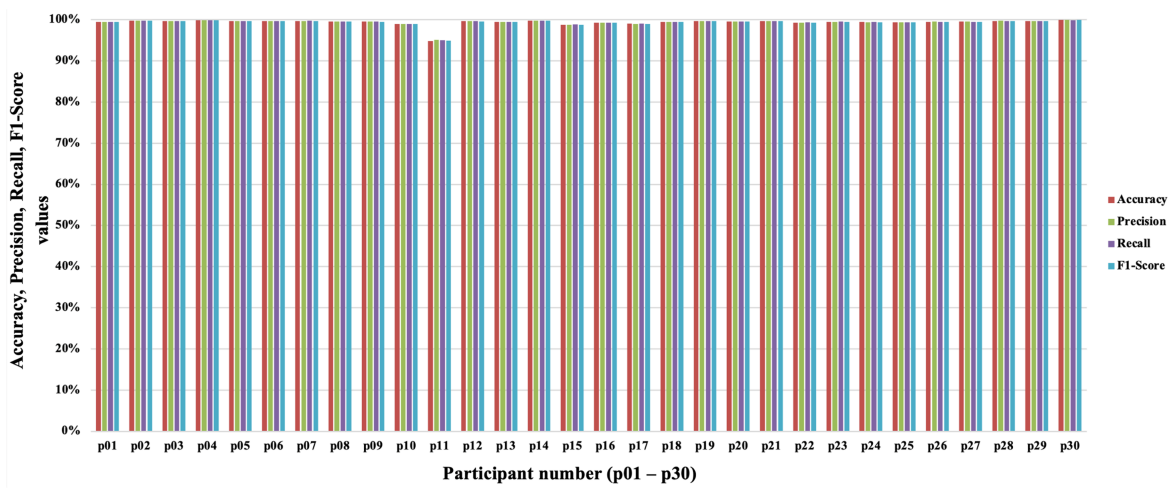
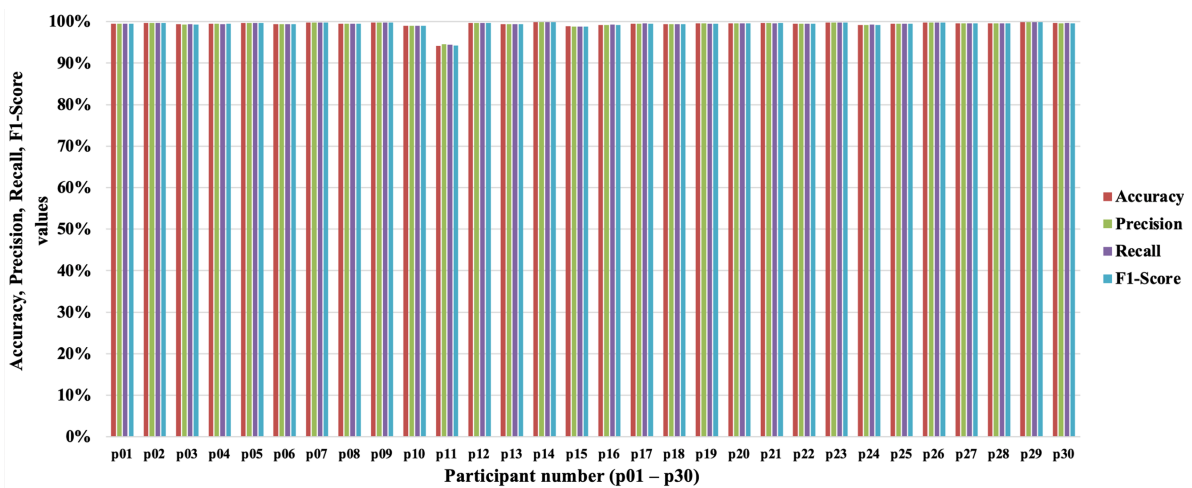


Figure 10
Representation of accuracy, precision, recall, and F1 score values in the 4th scenario



classification performance. Compared to previous scenarios, the application of relative differences yielded the most stable and accurate performance, underscoring the importance of implementing baseline reduction during EEG preprocessing, particularly in the six-movement recognition task.

A comparable trend was identified when integrating the multi-band feature matrix with the fractional difference approach (Figure 10). In this configuration, accuracy, precision, recall, and F1-score values approached 100% for most participants. This result confirms that the fractional difference can improve feature representation and EEG signals classification accuracy. Although fractional difference and relative difference both provide optimal performance, fractional difference combines the relative difference method with another method. Hence, the division of the relative difference method plays a crucial role in producing optimal features [13]. Overall, the comparison of the four scenarios shows that baseline reduction is an essential stage in EEG signals preprocessing, with the relative difference method producing the most stable and representative features (Tables 11–12).

Based on four test scenarios in Tables 11 and 12, it was concluded that the relative difference method produced more robust EEG signals features than the other two baseline reduction methods and the no-baseline approach. This finding aligns with Wirawan et al. [13]. Furthermore, the application of the relative and fractional difference methods has also been shown to yield lower loss values and epoch counts than the difference method, without the need for a baseline reduction approach. This finding demonstrates that the resulting features are easily recognized by the CNN, leading to lower loss values and fewer epochs.

In addition, the proposed method was validated on the public AMIGOS dataset to evaluate its reliability for extracting EEG signal features in a case study involving four emotion classes [18]. Table 13 compares the accuracy of this method with previous approaches. Based on Table 13, emotion recognition accuracy on the AMIGOS dataset shows significant variation, influenced by differences in preprocessing strategies, feature extraction, feature representation, and classification architecture. The power spectral density method with 2D topographical maps representation and CNN-based classification achieved 79.20% accuracy, due to

the loss of spatial information between EEG channels [19]. The z-score normalization and difference baseline reduction approach, integrated with CNN–LSTM, achieved 76.65% accuracy, slightly lower due to potential overfitting on a limited dataset [20]. Statistical methods such as mean (μ), standard deviation (σ), variance (σ^2), skewness, and kurtosis were also used for the EEG signals feature extraction process. Using the random forest method, emotion classification achieved 93.15% [21]. Furthermore, Zhao et al. [16] proposed a feature extraction process using convolution in the 2D CNN method. The results obtained in testing the AMIGOS dataset were 93.90% for four emotion classes.

Several studies have proposed a baseline reduction approach based on the difference method to improve the accuracy of EEG signals recognition, aiming to obtain more optimal feature representations. By using a 3D feature representation and a classification process with a CNN, accuracy rates of up to 95.95% have been achieved [22]. Further performance improvements were reported by Wirawan et al. [13] by combining MWMF, DE, and relative difference methods in the feature extraction stage. These features were then represented as 3D cubes and classified using a CNN, achieving an accuracy of 99.59%.

Although the approach developed by Wirawan et al. [13] demonstrated very high performance, the feature extraction process is still carried out separately. It has not been directly integrated into the classification architecture. In principle, within a CNN framework, the feature extraction process should be automated via convolution. Therefore, this study proposes an integrated framework that combines feature extraction, feature representation, and classification in a single processing pipeline by integrating relative difference methods, multi-band feature matrices, and CNNs. This proposed approach yields an average accuracy of 99.64%, indicating that the automated feature extraction process can produce more informative EEG features and that CNNs can more readily separate them during classification.

In general, integrating multi-band feature matrices with the relative difference approach yielded better results than traditional 2D and 3D representation techniques. Moreover, the relative difference strategy outperformed the standard difference method, aligning with results reported in earlier studies. In addition to

Table 11
Recapitulation of average accuracy, precision, recall, and F1-score values for all participants in each scenario

No	Scenarios	Accuracy (%)	Precision (%)	Recall (%)	F1-score (%)
1	Default	13,52	12,71	13,24	12,07
2	Difference	92,25	92,69	92,21	92,21
3	Relative difference	99,36	99,37	99,37	99,36
4	Fractional difference	99,36	99,37	99,36	99,35

Table 12
Recapitulation of average loss and epoch values for all participants in each scenario

No	Scenarios	Loss	Epochs
1	Default	1.8937	7.42
2	Difference	0.3165	21.76
3	Relative difference	0.0431	12.31
4	Fractional difference	0.0468	12.05

Table 13
Accuracy comparison between the proposed approach and prior studies using the AMIGOS dataset

No	Method	Accuracy (%)
1	Extraction feature: power spectral density. Feature representation: 2D topographical feature maps. Classification: CNN [19]	79.20
2	Preprocess: z-score norm. Baseline reduction: difference. Feature representation: 2D. Feature extraction and classification: CNN and Long Short-Term Memory (LSTM) [20]	76.65
3	Extraction feature: five statistical features. Representation features: 2D vector, Classification: random forest [21]	93.15
4	Baseline reduction: difference. Feature extraction and classification: 2D CNN [16]	93.90
5	Baseline reduction: difference. Feature representation: 3D cube. Feature extraction and classification: CNN [22]	95.95
6	Preprocess: MWMF, Extraction feature: DE. Representation features: 3D cube, Baseline reduction: relative difference. Classification: CNN [13]	99.59
7	Baseline reduction: relative difference. Feature representation: multi-band feature matrix. Extraction feature and classification: CNN (proposed)	99.64

its exceptional accuracy, the method proposed in this study also features a more concise processing pipeline than the method reported by Wirawan et al. [13].

4. Conclusion

This study proposes integrating relative difference baseline reduction with a multi-band feature matrix to generate optimal features for representing EEG signals characteristics. Using a CNN, this feature achieves high accuracy in classifying six motor movements. The multi-band feature matrix method explicitly utilizes information from four EEG frequency bands (theta, alpha, beta, and gamma), mapping them into a $9 \times 9 \times 512$ matrix to maintain spatial, frequency, and temporal dimensions simultaneously. The multi-band feature matrix method performs optimally when combined with the relative difference method, which reduces variations in EEG trial signal patterns across individuals. Testing on the MIMED dataset demonstrated very high and consistent classification performance across all evaluation metrics, such as loss, accuracy, precision, recall, F1-score, and number of epochs. Further validation on the public AMIGOS dataset for four-class emotion recognition achieved 99.64% accuracy, confirming the superiority of this method over previously reported techniques.

5. Limitations

Although the model proposed in this study demonstrates competitive performance in EEG-based movement activity recognition, several limitations remain. First, the model evaluation in this study was conducted only using ME data from the MIMED dataset. Consequently, the model's generalizability in the motor imagery (MI) domain, particularly in predicting six types of movement activities, has not been fully confirmed. Therefore, future research should examine the model's application and adaptation to MI data to assess the model's consistency and transferability in performance [17]. Second, the evaluation scheme is subject-dependent, with training and testing data from the same subject. While this approach captures specific usage conditions, the substantial variability of EEG signals across subjects may limit the model's generalizability. Therefore, further research is recommended to evaluate the model using a subject-independent approach to further evaluate its robustness and potential accuracy

gains in cross-subject scenarios [23, 24]. Third, model validation in this study is limited to the MIMED dataset and focuses on six specific movement activities. By leveraging transfer learning, future research can expand the scope of model evaluation to other datasets and a broader range of movement activities, thereby improving the model's adaptability across domains and tasks [25]. Fourth, the proposed model is currently implemented in an offline scenario, so it is not yet capable of predicting movement activities in real time. To support implementation in real-world environments, further research needs to integrate a lab streaming layer architecture or a data stream-based processing framework to enable inference directly from incoming EEG signals. This development opens opportunities for integrating models into Internet of Things devices, such as exoskeletons, to support mobility for people with disabilities [26]. Fifth, although the CNN-based classification method used in this study achieves high accuracy, this architecture still has limitations in preserving spatial information from EEG features during the flattening stage. In this process, the feature representation in matrix form is reduced to a scalar, potentially losing the spatial relationships between feature elements. Therefore, further research is needed to examine the application of classification methods that explicitly preserve and model spatial structure during inference, such as capsule networks, which are designed to represent hierarchical and spatial relationships between features more effectively [27]. Sixth, although the proposed relative difference method and multi-band feature matrix are effective in generating discriminatory features, residual artifacts in the EEG signals cannot be completely eliminated. Therefore, future research should focus on developing more robust artifact reduction techniques that can more effectively suppress EEG artifacts while preserving the underlying neurophysiological patterns [13].

Acknowledgments

The authors are grateful to the student member of the Data Science Lab at Universitas Pendidikan Ganesha, Indonesia, for assistance with data analysis.

Funding Support

This research was fully funded under the 2025 Fiscal Year Grant (No. 346/UN48.16/PT/2025) provided by the Directorate

of Research, Technology, and Community Service, Ministry of Higher Education, Science, and Technology, Indonesia.

Ethical Statement

The data used in this study were obtained from publicly available and fully de-identified sources: the MIMED dataset (Mendeley Data, DOI: [10.17632/zs25xxjkmj.3](https://doi.org/10.17632/zs25xxjkmj.3)) and the AMIGOS dataset (Miranda-Correa et al. [18]; DOI: [10.1109/TAFFC.2018.2884461](https://doi.org/10.1109/TAFFC.2018.2884461)). No new experiments or data collection involving human participants were conducted by the authors. The datasets were originally collected by their respective providers under approved institutional ethical protocols with written informed consent from all participants. Therefore, ethical approval and informed consent were not required for the present study.

Conflicts of Interest

The authors declare that they have no conflicts of interest to this work.

Data Availability Statement

The MIMED dataset that supports the findings of this study is openly available in Mendeley Data at <https://data.mendeley.com/datasets/zs25xxjkm9/3>. The AMIGOS dataset that supports the findings of this study is openly available at <https://doi.org/10.1109/TAFFC.2018.2884461>, reference number [18].

Author Contribution Statement

I Made Agus Wirawan: Conceptualization, Methodology, Software, Validation, Formal analysis, Investigation, Resources, Data curation, Writing – original draft, Writing – review & editing, Visualization, Supervision, Project administration, Funding acquisition. **I Nyoman Sukajaya:** Methodology, Software, Validation, Formal analysis, Investigation, Resources, Data curation, Writing – original draft, Writing – review & editing, Visualization, Project administration. **Ni Nyoman Mestri Agustini:** Methodology, Validation, Formal analysis, Investigation, Writing – original draft, Writing – review & editing, Visualization, Supervision, Project administration.

References

- [1] Hameed, I., Khan, D. M., Ahmed, S. M., Aftab, S. S., & Fazal, H. (2025). Enhancing motor imagery EEG signal decoding through machine learning: A systematic review of recent progress. *Computers in Biology and Medicine*, 185, 109534. <https://doi.org/10.1016/j.compbiomed.2024.109534>
- [2] Altaheri, H., Muhammad, G., Alsulaiman, M., Amin, S. U., Altuwaijri, G. A., Abdul, W., . . . , & Faisal, M. (2023). Deep learning techniques for classification of electroencephalogram (EEG) motor imagery (MI) signals: A review. *Neural Computing and Applications*, 35, 14681–14722. <https://doi.org/10.1007/s00521-021-06352-5>
- [3] Singh, A., Hussain, A. A., Lal, S., & Guesgen, H. W. (2021). A comprehensive review on critical issues and possible solutions of motor imagery based electroencephalography brain-computer interface. *Sensors*, 21(6), 2173. <https://doi.org/10.3390/s21062173>
- [4] Lazarou, I., Nikolopoulos, S., Petrantonakis, P. C., Kompatisaris, I., & Tsolaki, M. (2018). EEG-based brain-computer interfaces for communication and rehabilitation of people with motor impairment: A novel approach of the 21st century. *Frontiers in Human Neuroscience*, 12, 14. <https://doi.org/10.3389/fnhum.2018.00014>
- [5] Kumar, A., Gao, L., Li, J., Ma, J., Fu, J., Gu, X., . . . , & Fang, Q. (2022). Error-related negativity-based robot-assisted stroke rehabilitation system: Design and proof-of-concept. *Frontiers in Neurobotics*, 16, 837119. <https://doi.org/10.3389/fnbot.2022.837119>
- [6] Sun, C., & Mou, C. (2023). Survey on the research direction of EEG-based signal processing. *Frontiers in Neuroscience*, 17, 1203059. <https://doi.org/10.3389/fnins.2023.1203059>
- [7] Wang, X., Liesaputra, V., Liu, Z., Wang, Y., & Huang, Z. (2024). An in-depth survey on deep learning-based motor imagery electroencephalogram (EEG) classification. *Artificial Intelligence in Medicine*, 147, 102738. <https://doi.org/10.1016/j.artmed.2023.102738>
- [8] Mohammad, A., Siddiqui, F., & Alam, M. A. (2021). Feature extraction from EEG signals: A deep learning perspective. In *2021 11th International Conference on Cloud Computing, Data Science & Engineering*, 757–760. <https://doi.org/10.1109/Confluence51648.2021.9377108>
- [9] Huang, H., Deng, Y., Hao, B., Liu, W., Tu, X., & Zeng, G. (2025). Emotion recognition method using U-Net neural network with multichannel EEG features and differential entropy characteristics. *IEEE Access*, 13, 59377–59389. <https://doi.org/10.1109/ACCESS.2024.3497160>
- [10] Patel, P., Raghunandan, R., & Annavarapu, R. N. (2021). EEG-based human emotion recognition using entropy as a feature extraction measure. *Brain Informatics*, 8(1), 20. <https://doi.org/10.1186/s40708-021-00141-5>
- [11] Sasatake, Y., & Matsushita, K. (2025). EEG baseline analysis for effective extraction of P300 event-related potentials for welfare interfaces. *Sensors*, 25(10), 3102. <https://doi.org/10.3390/s25103102>
- [12] Yang, Y., Wu, Q., Fu, Y., & Chen, X. (2018). Continuous convolutional neural network with 3D input for EEG-based emotion recognition. In *Neural Information Processing: 25th International Conference*, 433–443. https://doi.org/10.1007/978-3-030-04239-4_39
- [13] Wirawan, I. M. A., Wardoyo, R., Lelono, D., & Kusrohmaniah, S. (2022). Modified weighted mean filter to improve the baseline reduction approach for emotion recognition. *Emerging Science Journal*, 6(6), 1255–1273. <https://doi.org/10.28991/ESJ-2022-06-06-03>
- [14] Shah, D., Gopan, K. G., & Sinha, N. (2022). An investigation of the multi-dimensional (1D vs. 2D vs. 3D) analyses of EEG signals using traditional methods and deep learning-based methods. *Frontiers in Signal Processing*, 2, 936790. <https://doi.org/10.3389/frsip.2022.936790>
- [15] Yuvaraj, R., Baranwal, A., Prince, A. A., Murugappan, M., & Mohammed, J. S. (2023). Emotion recognition from spatio-temporal representation of EEG signals via 3D-CNN with ensemble learning techniques. *Brain Sciences*, 13(4), 685. <https://doi.org/10.3390/brainsci13040685>
- [16] Zhao, Y., Liu, S., Cao, L., Ji, Y., Wu, W., & Wang, B. (2026). Electrode quantity outperforms spatial topology in EEG-based emotion recognition: A dual-CNN study on electrode configuration. *Biomedical Signal Processing and Control*, 113, 109082. <https://doi.org/10.1016/j.bspc.2025.109082>
- [17] Wirawan, I. M. A., Maneetham, D., Darmawiguna, I. G. M., Niyomphol, A., Sawetmethikul, P., Crisnapati, P. N., . . . ,

- & Agustini, N. N. M. (2024). Acquisition and processing of motor imagery and motor execution dataset (MIMED) for six movement activities. *Data in Brief*, 56, 110833. <https://doi.org/10.1016/j.dib.2024.110833>
- [18] Miranda-Correa, J. A., Abadi, M. K., Sebe, N., & Patras, I. (2018). AMIGOS: A dataset for affect, personality and mood research on individuals and groups. *IEEE Transactions on Affective Computing*, 12(2), 479–493. <https://doi.org/10.1109/TAFFC.2018.2884461>
- [19] Aguiñaga, A. R., Ramirez, M. R., Soto, M. D. C. S., & Cisnero, M. D. L. A. Q. (2024). A multimodal low complexity neural network approach for emotion recognition. *Human Behavior and Emerging Technologies*, 2024(1), 5581443. <https://doi.org/10.1155/2024/5581443>
- [20] Dar, M. N., Akram, M. U., Khawaja, S. G., & Pujari, A. N. (2020). CNN and LSTM-based emotion charting using physiological signals. *Sensors*, 20(16), 4551. <https://doi.org/10.3390/s20164551>
- [21] Kumar, A., & Kumar, A. (2025). Human emotion recognition using machine learning techniques based on the physiological signal. *Biomedical Signal Processing and Control*, 100, 107039. <https://doi.org/10.1016/j.bspc.2024.107039>
- [22] Zhao, Y., Yang, J., Lin, J., Yu, D., & Cao, X. (2020). A 3D convolutional neural network for emotion recognition based on EEG signals. In *2020 International Joint Conference on Neural Networks*, 1–6. <https://doi.org/10.1109/IJCNN48605.2020.9207420>
- [23] Jia, X., Song, Y., & Xie, L. (2023). Excellent fine-tuning: From specific-subject classification to cross-task classification for motor imagery. *Biomedical Signal Processing and Control*, 79, 104051. <https://doi.org/10.1016/j.bspc.2022.104051>
- [24] Feng, J., Li, Y., Jiang, C., Liu, Y., Li, M., & Hu, Q. (2022). Classification of motor imagery electroencephalogram signals by using adaptive cross-subject transfer learning. *Frontiers in Human Neuroscience*, 16, 1068165. <https://doi.org/10.3389/fnhum.2022.1068165>
- [25] Liang, H.-J., Li, L.-L., & Cao, G.-Z. (2024). FDCN-C: A deep learning model based on frequency enhancement, deformable convolution network, and crop module for electroencephalography motor imagery classification. *PLOS One*, 19(11), e0309706. <https://doi.org/10.1371/journal.pone.0309706>
- [26] Sarhan, S. M., Al-Faiz, M. Z., & Takhakh, A. M. (2023). A review on EMG/EEG based control scheme of upper limb rehabilitation robots for stroke patients. *Heliyon*, 9(8), e18308. <https://doi.org/10.1016/j.heliyon.2023.e18308>
- [27] Wirawan, I. M. A., Aryanto, K. Y. E., Sukajaya, I. N., Agustini, N. N. M., & Putri, D. A. W. M. (2025). Hybrid method for optimizing emotion recognition models on electroencephalogram signals. *IAES International Journal of Artificial Intelligence*, 14(3), 2302–2314. <https://doi.org/10.11591/ijai.v14.i3.pp2302-2314>

How to Cite: Wirawan, I. M. A., Sukajaya, I. N., & Agustini, N. N. M. (2026). Optimization of Electroencephalogram Feature Based on Multi-Band Feature Matrix and Relative Difference for Imagined Motor Movement Pattern Classification. *Journal of Computational and Cognitive Engineering*. <https://doi.org/10.47852/bonviewJCCE62027142>